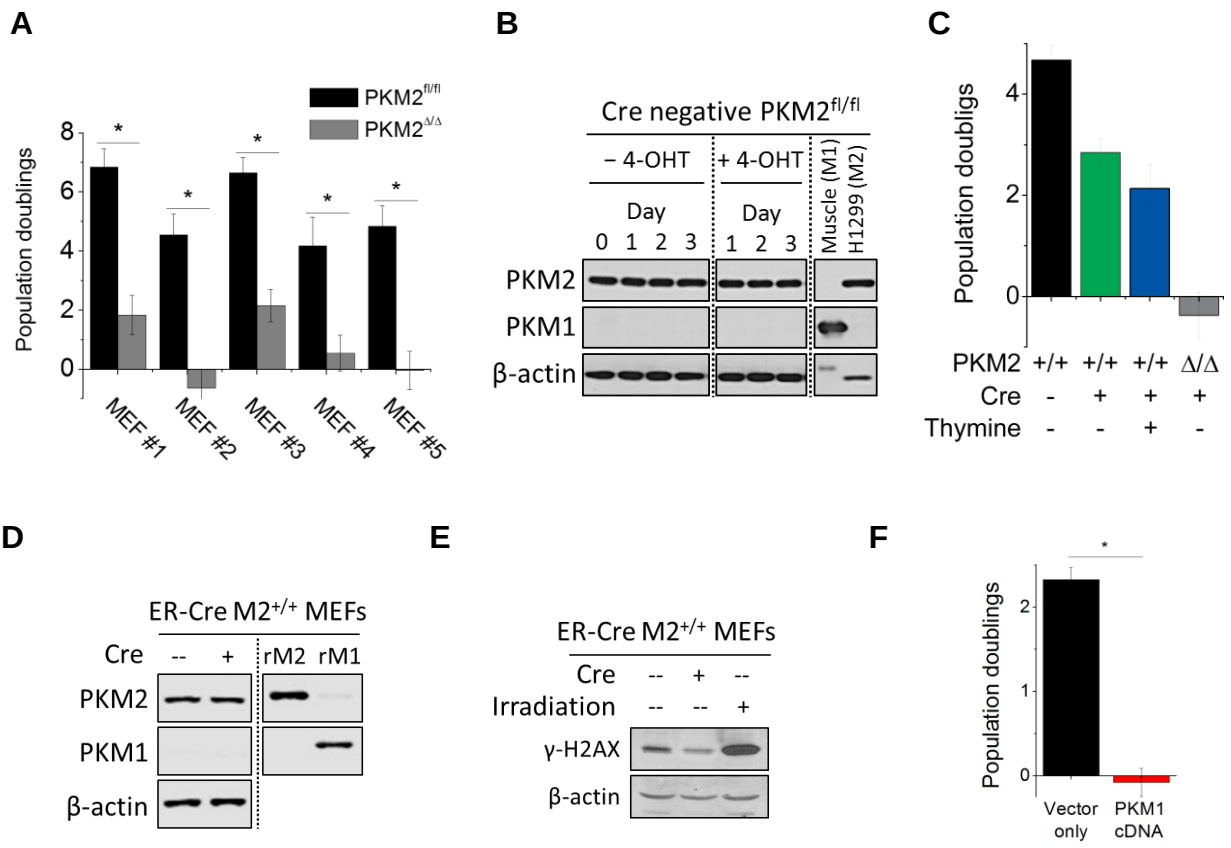

Figure S1. Proliferation arrest in MEFs isolated from different mice, related to Figure 1.

(A) Population doublings over 10 days of *PKM2*$^{\Delta/\Delta}$ MEFs generated from five different *PKM2*$^{fl/fl}$ *Cre-ER* mice following vehicle or 4-hydroxytamoxifen (4-OHT) treatment of *PKM2*$^{fl/fl}$ MEFs. Data are displayed as means ± SEM, n=3 (*p < 0.05).

(B) Western blot analysis of Cre negative *PKM2*$^{fl/fl}$ MEFs following vehicle or 4-OHT treatment. Western blots of lysate from mouse muscle or H1299 cancer cells are included as controls for PKM1 and PKM2 expression, respectively.

(C) Population doublings over 10 days of MEFs generated from *PKM2*$^{+/+}$ *Cre-ER* mice following vehicle, 4-hydroxytamoxifen (4-OHT), or 4-OHT plus 250 µM thymine supplementation. *PKM2*$^{\Delta/\Delta}$ MEFs generated from *PKM2*$^{fl/fl}$ *Cre-ER* mice following 4-OHT treatment are also shown for comparison. Data are displayed as means ± SEM, n=3.

(D) Western blot analysis of MEFs generated from *PKM2*$^{+/+}$ *Cre-ER* mice. 4-OHT treatment does not affect pyruvate kinase isoform expression. Western blot analysis of 100 ng of recombinant PKM1 or PKM2 (rPKM1, rPKM2) are included as controls.

(E) Western blot analysis of MEFs generated from *PKM2*$^{+/+}$ *Cre-ER* mice with vehicle or 4-OHT treatment. Irradiated MEFs are included as controls.

(F) Population doublings over 10 days of wildtype MEFs with pLHCX vector only or with exogenous expression of PKM1 cDNA. Data are displayed as means ± SEM, n=3 (*p < 0.05).

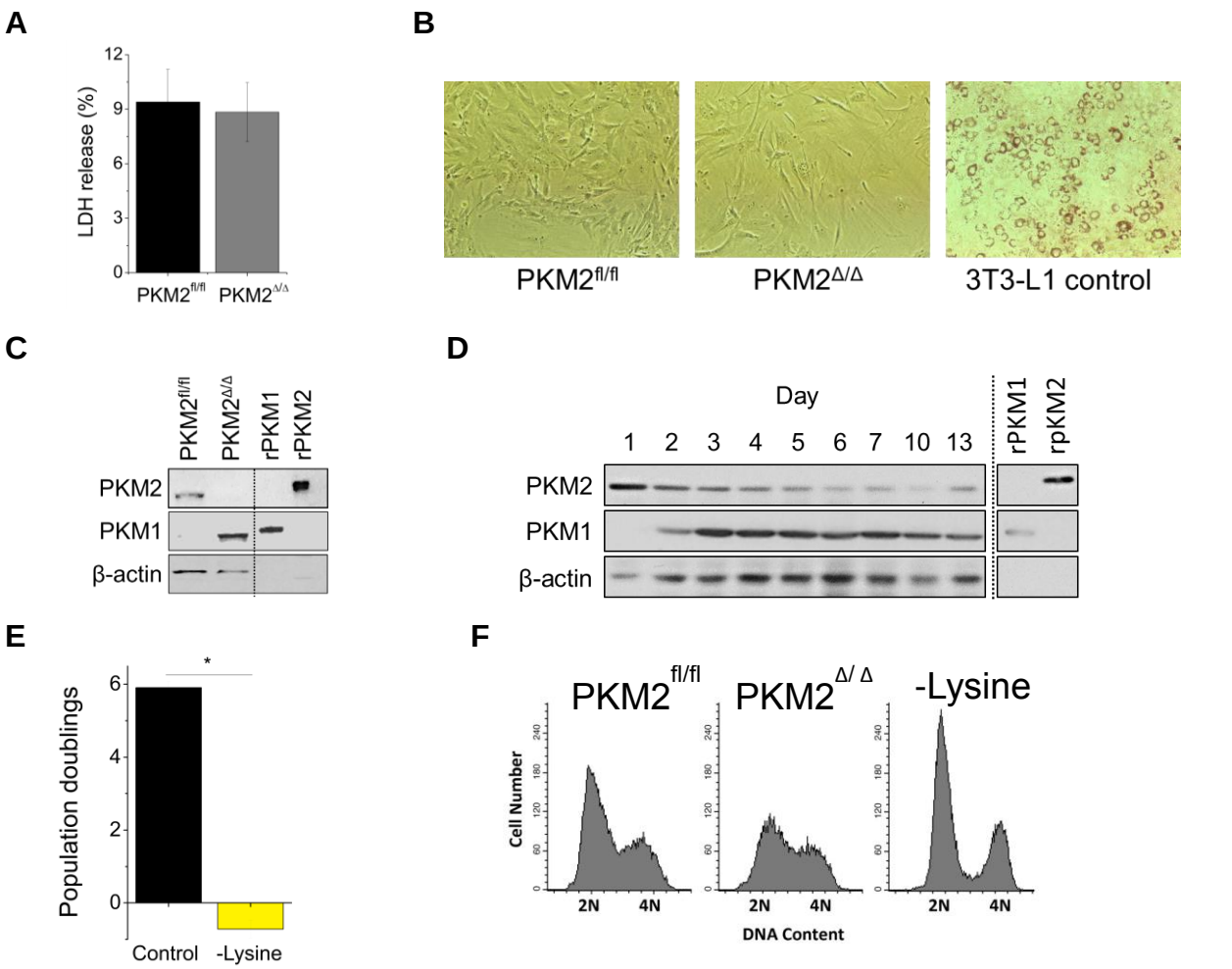

Figure S2. *PKM2*$^{\Delta/\Delta}$ cells undergo proliferation arrest without cell death or differentiation, and the arrest is different from cell cycle arrest triggered by nutrient deprivation, related to Figure 2.

(A) Quantification of cell death over a 24 h period by LDH release after treatment of *PKM2*$^{fl/fl}$ MEFs with vehicle (*PKM2*$^{fl/fl}$) or 4-OHT (*PKM2*$^{\Delta/\Delta}$). Data are displayed as means ± SEM, n=3.

(B) Oil Red O staining of *PKM2*$^{fl/fl}$ and *PKM2*$^{\Delta/\Delta}$ MEFs 6 days after treatment with vehicle or 4-OHT. The right pane shows a positive control of wildtype immortalized MEFs differentiated into adipocytes by expression of PPARγ.

(C) Western blot analysis of *PKM2*$^{fl/fl}$ and *PKM2*$^{\Delta/\Delta}$ myoblasts 9 days after treatment with vehicle or 4-OHT.

(D) Western blot analysis of primary myoblasts following incubation in low-serum media to induce differentiation into myotubes. Western blot analysis of 100 ng of recombinant PKM1 or PKM2 (rPKM1, rPKM2) are included as controls for both panels.

(E) Population doublings over 10 days of MEFs generated from wildtype mice in regular DMEM media or DMEM media without lysine. Data are displayed as means ± SEM, n=3 (*$p < 0.05$).

(F) DNA content was assessed using propidium iodide staining and flow cytometry in *PKM2*$^{fl/fl}$ MEFs, *PKM2*$^{\Delta/\Delta}$ MEFs, and MEFs cultured in media without lysine.

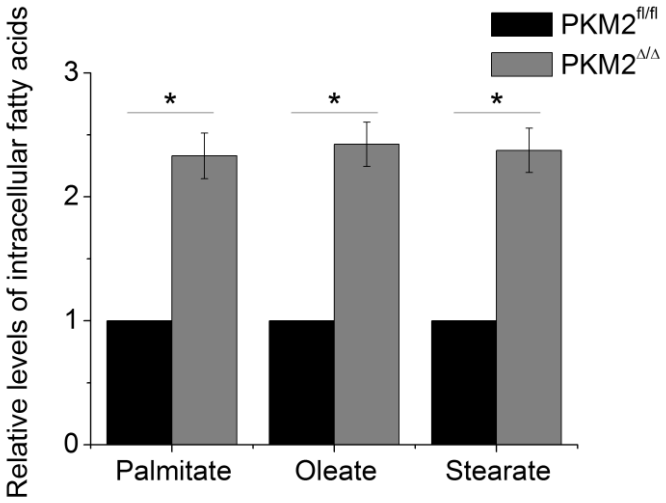

Figure S3. Levels of intracellular fatty acids, related to Figure 3. Fatty acids were extracted from *PKM2*$^{fl/fl}$ and *PKM2*$^{\Delta/\Delta}$ MEFs 7 days after treatment of *PKM2*$^{fl/fl}$ MEFs with vehicle or 4-OHT. All data are displayed as means ± SEM, n=3 (*p < 0.05).

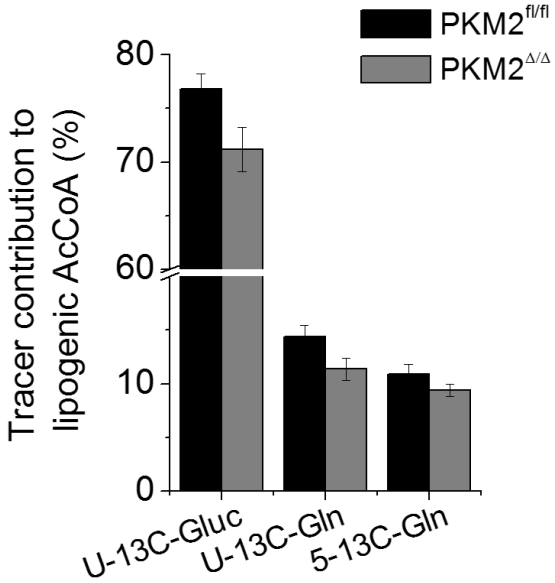

Figure S4. Less palmitate is synthesized from glucose and glutamine in *PKM2*$^{\Delta/\Delta}$ MEFs relative to *PKM2*$^{fl/fl}$ MEFs, related to Figure 4. The relative contribution of [U-^{13}C]glucose, [U-^{13}C]glutamine, and [5-^{13}C]glutamine to newly synthesized palmitate in *PKM2*$^{fl/fl}$ and *PKM2*$^{\Delta/\Delta}$ MEFs 7 days after *PKM2*$^{fl/fl}$ *Cre-ER* MEFs were treated with vehicle or 4-OHT was determined as described previously (Fendt et al., 2013; Metallo et al., 2012). Data are displayed as means ± SEM, n=3 (*p < 0.05).

A

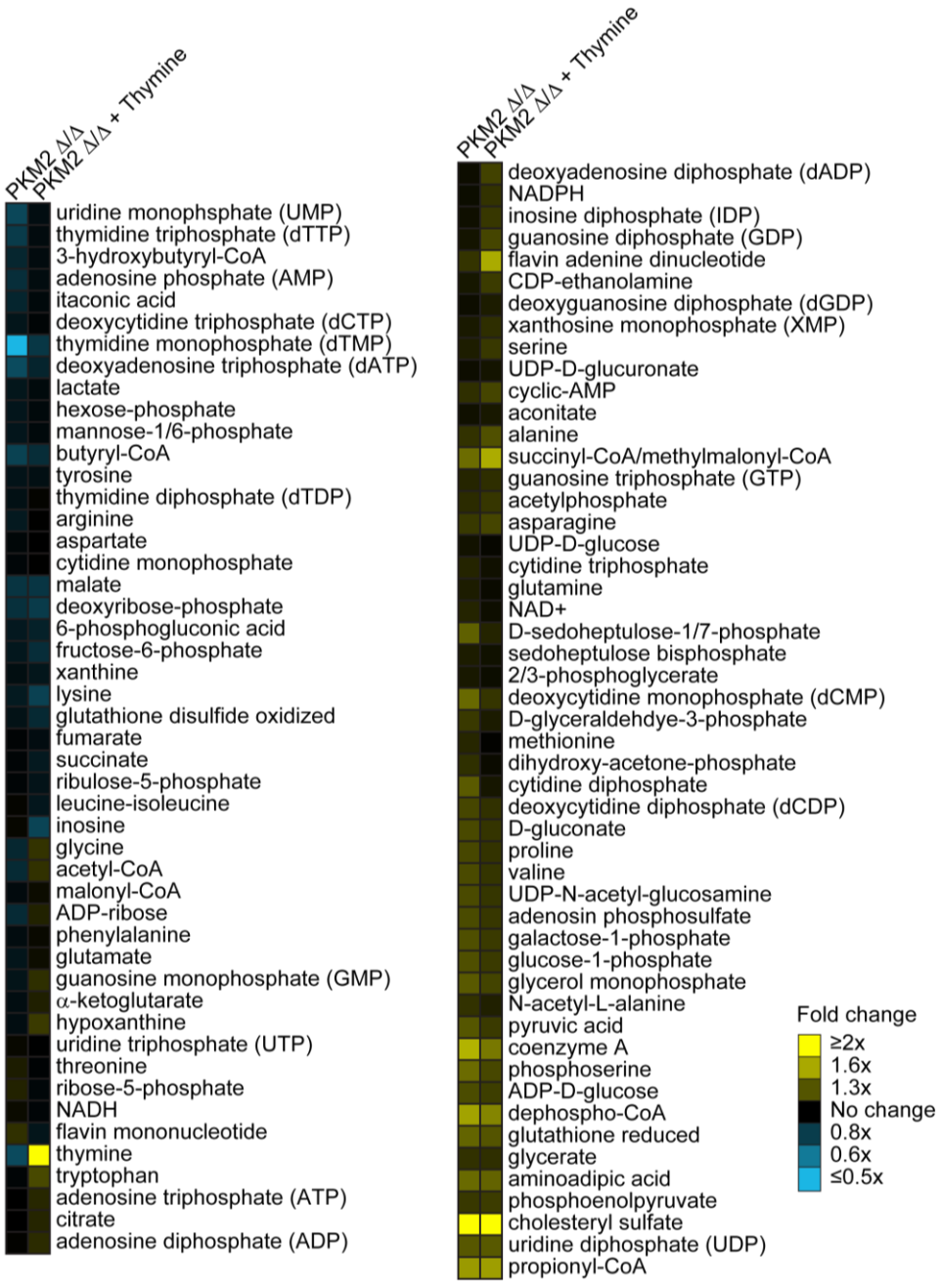
PKM2 Δ/Δ
PKM2 Δ/Δ + Thymine
uridine monophsphate (UMP)
thymidine triphosphate (dTTP)
3-hydroxybutyryl-CoA
adenosine phosphate (AMP)
itaconic acid
deoxycytidine triphosphate (dCTP)
thymidine monophosphate (dTMP)
deoxyadenosine triphosphate (dATP)
lactate
hexose-phosphate
mannose-1/6-phosphate
butyryl-CoA
tyrosine
thymidine diphosphate (dTDP)
arginine
aspartate
cytidine monophosphate
malate
deoxyribose-phosphate
6-phosphogluconic acid
fructose-6-phosphate
xanthine
lysine
glutathione disulfide oxidized
fumarate
succinate
ribulose-5-phosphate
leucine-isoleucine
inosine
glycine
acetyl-CoA
malonyl-CoA
ADP-ribose
phenylalanine
glutamate
guanosine monophosphate (GMP)
α-ketoglutarate
hypoxanthine
uridine triphosphate (UTP)
threonine
ribose-5-phosphate
NADH
flavin mononucleotide
thymine
tryptophan
adenosine triphosphate (ATP)
citrate
adenosine diphosphate (ADP)
PKM2 Δ/Δ
PKM2 Δ/Δ + Thymine
deoxyadenosine diphosphate (dADP)
NADPH
inosine diphosphate (IDP)
guanosine diphosphate (GDP)
flavin adenine dinucleotide
CDP-ethanolamine
deoxyguanosine diphosphate (dGDP)
xanthosine monophosphate (XMP)
serine
UDP-D-glucuronate
cyclic-AMP
aconitate
alanine
succinyl-CoA/methylmalonyl-CoA
guanosine triphosphate (GTP)
acetylphosphate
asparagine
UDP-D-glucose
cytidine triphosphate
glutamine
NAD+
D-sedoheptulose-1/7-phosphate
sedoheptulose bisphosphate
2/3-phosphoglycerate
deoxycytidine monophosphate (dCMP)
D-glyceraldehdye-3-phosphate
methionine
dihydroxy-acetone-phosphate
cytidine diphosphate
deoxycytidine diphosphate (dCDP)
D-gluconate
proline
valine
UDP-N-acetyl-glucosamine
adenosin phosphosulfate
galactose-1-phosphate
glucose-1-phosphate
glycerol monophosphate
N-acetyl-L-alanine
pyruvic acid
coenzyme A
phosphoserine
ADP-D-glucose
dephospho-CoA
glutathione reduced
glycerate
aminoadipic acid
phosphoenolpyruvate
cholesteryl sulfate
uridine diphosphate (UDP)
propionyl-CoA
Fold change
≥2x
1.6x
1.3x
No change
0.8x
0.6x
≤0.5x

B

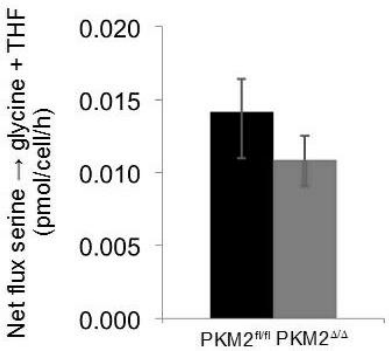
Net flux serine → glycine + THF
(pmol/cell/h)
0.020
0.015
0.010
0.005
0.000
PKM2fl/fl PKM2Δ/Δ

Figure S5. Pyruvate kinase isoform expression affects cellular metabolism, related to Figure 5.

(A) Profiles of intracellular metabolites in *PKM2*$^{\Delta/\Delta}$ MEFs without or with 250 μM thymine supplementation 7 days after treatment of *PKM2*$^{fl/fl}$ MEFs with vehicle or 4-OHT, as determined by GC-MS or LC-MS/MS. Relative levels are expressed as the log ratio of the normalized signal intensity in *PKM2*$^{\Delta/\Delta}$ MEFs to the normalized signal intensity in the *PKM2*$^{fl/fl}$ MEFs. Signal intensity was also normalized by total protein content to account for the difference in size between *PKM2*$^{fl/fl}$ and *PKM2*$^{\Delta/\Delta}$ MEFs (n=3).

(B) Net serine to glycine and THF flux in PKM2$^{fl/fl}$ and PKM2$^{\Delta/\Delta}$ MEFs. Fluxes were modeled based on ^{13}C glucose labeling in serine and glycine and the serine and glycine uptake rates. Differences between PKM2$^{fl/fl}$ and PKM2$^{\Delta/\Delta}$ MEFs are not significant based on 95% confidence intervals.

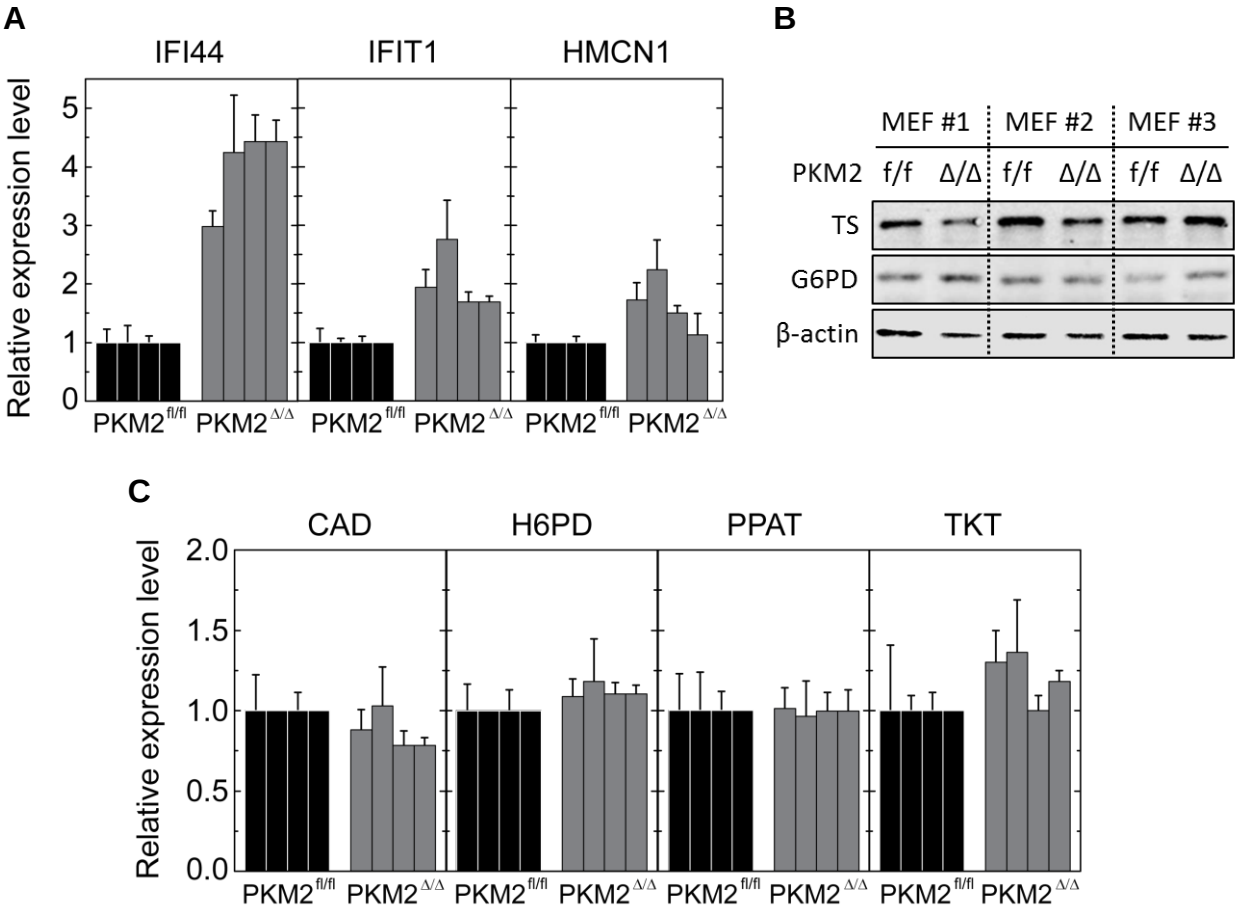

Figure S6. Expression analysis of select genes and proteins, related to Figure 6.
(A) Quantitative RT-PCR results for genes identified to have the largest difference in gene expression from analysis using Affymetrix GeneChip Mouse Gene 1.0 ST array: Interferon Induced Protein 44 (IFI44); Interferon-Induced Protein With Tetratricopeptide Repeats 1 (IFIT1); Hemicentin 1 (HMCN1). RNA was isolated from *PKM2*$^{fl/fl}$ and *PKM2*$^{\Delta/\Delta}$ MEFs derived from four independent *PKM2*$^{fl/fl}$ *Cre-ER* embryos 7 days following vehicle or 4-OHT addition. Data are displayed as means ± SEM, n=3.
(B) Western blot analysis of protein lysates from *PKM2*$^{fl/fl}$ and *PKM2*$^{\Delta/\Delta}$ MEFs derived from three independent *PKM2*$^{fl/fl}$ *Cre-ER* embryos for enzymes involved in nucleotide biosynthesis: thymidylate synthase (TS); Glucose-6-phosphate dehydrogenase (G6PD). *PKM2*$^{fl/fl}$ *Cre-ER* MEFs were treated with 4-OHT (*PKM2*$^{\Delta/\Delta}$) or vehicle (*PKM2*$^{fl/fl}$) for 7 days before collecting protein lysates.
(C) Quantitative RT-PCR results for genes involved in nucleotide biosynthesis: Carbamoyl-Phosphate Synthetase 2, Aspartate Transcarbamylase, and Dihydroorotase (CAD); Glucose-6-Phosphate Dehydrogenase (H6PD); Phosphoribosyl Pyrophosphate Amidotransferase (PPAT); Transketolase (TKT). RNA was isolated from *PKM2*$^{fl/fl}$ and *PKM2*$^{\Delta/\Delta}$ MEFs derived from four independent *PKM2*$^{fl/fl}$ *Cre-ER* embryos 7 days following vehicle or 4-OHT addition. Data are displayed as means ± SEM, n=3.

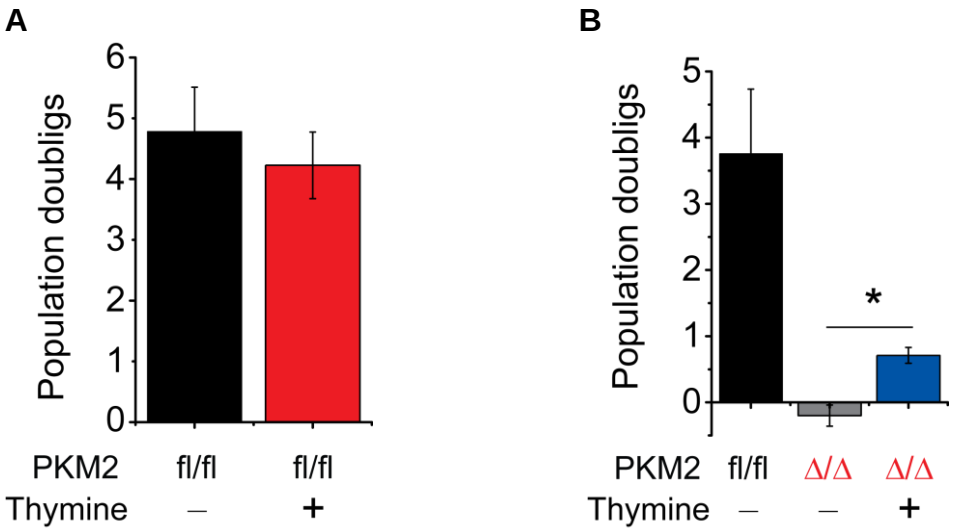

Figure S7. Exogenous thymine supplementation affects *PKM2*$^{\Delta/\Delta}$, but not *PKM2*$^{fl/fl}$, MEF proliferation, related to Figure 7.

(A) Population doublings over 10 days of *PKM2*$^{fl/fl}$ MEFs were measured with or without thymine supplemented in the media at a concentration of 250 μM. Data are displayed as means ± SEM, n=3.

(B) Population doublings over 10 days of *PKM2*$^{fl/fl}$ and *PKM2*$^{\Delta/\Delta}$ MEFs. 250 μM thymine was added on day 5 after addition of 4-OHT when *PKM2*$^{\Delta/\Delta}$ MEFs had stopped proliferating. All proliferation of *PKM2*$^{\Delta/\Delta}$ MEFs occurred between day 5 and 10 after thymine addition. Data are displayed as means ± SEM, n=3. *The difference in population doubling of *PKM2*$^{\Delta/\Delta}$ MEFs with and without thymine supplementation is statistically significant ($p < 0.05$).

Table S1 included as Excel spreadsheet. Mass isotopomer distributions (MIDs) of measured intracellular metabolites, related to Figure 5. MIDs of all metabolites were measured by GCMS, except for MIDs of UMP and hexose phosphate, which were measured by LC-MS/MS. Numbers shown are average fraction of each isotopomer ± SEM, n=3. MIDs have been corrected for natural isotope abundance.

Table S2 included as Excel spreadsheet. Mass isotopomer distributions (MIDs) of measured intracellular metabolites over time, related to Figure 5. MIDs of all metabolites were measured by LC-MS/MS. Numbers shown are average fraction of each isotopomer ± SEM, n=3. MIDs have been corrected for natural isotope abundance.

SUPPLEMENTAL EXPERIMENTAL PROCEDURES

All mouse studies were performed in accordance with institutional guidelines and approved by the MIT committee on animal care.

Isolation and culture of primary mouse embryonic fibroblasts

Primary mouse embryonic fibroblasts (MEFs) were isolated and cultured using an adaption of previously published methods (Springer et al., 2001). Embryos were isolated from the uterus of pregnant mice staged E11.5 – E14.5 of gestation and decapitated in PBS. Each embryo was processed separately due to heterogeneity in genetic background. After removing blood and organ tissue from each embryo, each was homogenized, resuspended in 2 ml of 0.25% warm trypsin, and incubated at 37°C for 30 min. To break up genomic DNA, 5 ml of HBSS with $CaCl_2$ and $MgCl_2$ was first added to each tube, and treated with 5 µl of $5\mu g \cdot \mu l^{-1}$ DNase. The mixture was incubated at 37°C for 5 - 15 min. The supernatant was collected and transferred to a fresh tube on ice. Additional 2 ml of 0.25% trypsin was added to the remaining tissue pieces and incubated at 37°C for 30 min and again treated with HBSS and DNase. The supernatant was collected and added to the previous tube of cells on ice. Cells were pelleted, resuspended in MEF medium (Dulbecco's Modified Eagle's Medium with 10% heat inactivated FBS, 1% streptomycin/penicillin, 1 mM glutamine, and 0.1 mM 2-mercaptoethanol) and plated at a density of 5×10^6 cells per 10 cm plate. Cells were split before reaching confluence and replated at 750,000 cells per 10 cm plate, or frozen in 3×10^6 cell aliquots. 1 µM 4-hydroxytamoxifen dissolved in ethanol was used to induce recombination of *PKM2*^{fl} alleles. Cells starved of lysine were incubated in lysine-free DMEM and doubling time analyzed over 10 days.

Isolation and culture of primary myoblasts

Primary myoblasts were isolated and cultured using an adaptation of previously published methods (Rando and Blau, 1994; Springer et al., 2001). Muscle was isolated from 2 – 2.5 week old mice and mechanically disaggregated, followed by enzymatic disaggregation with Collagenase P (10 $mg \cdot ml^{-1}$ in PBS; Roche) at 37°C for 45 min with trituration every 15 min. The slurry was passed through a 70µm filter, and additional PBS was added to dilute out collagenase. Cells were pelleted by centrifugation and pre-plated on a non-treated tissue culture plate for 4 h to remove fibroblasts. Unattached myoblasts were re-plated in 0.1% gelatin coated plates in F-10-based primary myoblast growth medium (Ham's F10 medium with 10% Cosmic calf serum (Hyclone), 1% streptomycin/penicillin, 1 mM glutamine, and 2.5 $ng \cdot ml^{-1}$ basic fibroblast growth factor (PeproTech)). Medium was changed every 2 days, and cells were split before reaching confluence, at no more than 1:5 dilution. Myoblasts are capable of differentiation into myotubes when cultured under conditions that promote differentiation (Springer et al., 2001). For differentiation into myotubes, cells were cultured in low-serum medium: Dulbecco's Modified Eagle's Medium with 5% horse serum, 1% streptomycin/penicillin, and 1 mM glutamine. Medium was changed daily. To prepare gelatin coated plates, 2% gelatin stock (Sigma-Aldrich) was warmed up to 37°C and diluted to a concentration of 0.1% in PBS. Approximately 7 ml of the diluted 0.1% gelatin solution in PBS was added to each 10 cm plate and incubated at 37°C for at

least 1 h. The gelatin solution was aspirated, and plates were rinsed with fresh PBS before use.

Cell lysis and immunoblotting

Cell lysis and Western blot analysis were carried out according to standard protocols. The following dilutions of primary commercial antibodies were used as probes: 1:20000 dilution of anti-PKM1 (Sigma SAB4200094); 1:10000 dilution of anti-PKM2 (Cell Signaling 4053S); 1:500 dilution of anti-actin (Abcam ab8226); 1:1000 dilution of anti-γ-H2AX (EMD Millipore 05-636); 1:1000 dilution of anti-TS (Cell Signaling 9045); and 1:1000 dilution of anti-G6PD (Cell Signaling 12263). Primary antibodies were diluted in 5% BSA containing 0.1% azide and incubated overnight at 4°C. Secondary antibodies were diluted in 5% BSA at a dilution of 1:10000.

Cell cycle analysis

Cells were centrifuged at 1000g for 5 minutes and washed twice in PBS. The cell pellet was resuspended in 500 µl of ice-cold PBS. To fix the cells, 5 ml of ice cold ethanol was added to the cell suspension. Cells were fixed at 4°C at least overnight. Just before analysis, fixed cells were centrifuged at 1000g and washed twice in PBS with 1% BSA. Cells were treated with RNase and resuspended in the wash buffer with propidium iodide added to a final concentration of 50 $\mu g \cdot ml^{-1}$. Cells were analyzed for propidium iodide (JM-1056, from MBL Int'l.) content on a Becton Dickinson FACScan flow cytometer; a laser with wavelength 488 nm was used for excitation and emission measured at 585 nm. To assay for new DNA synthesis, the Click-iT EdU Alexa Fluor 488 kit was used (Invitrogen C35002). 10 µM of EdU was used for a 3 hour incubation. Cells were imaged on a Nikon Eclipse TE2000-U microscope with a 4 second exposure time and analyzed using the ImageJ software. Cells were dual stained for DNA content and new DNA synthesis with the Click-iT EdU Alexa Fluor 488 Kit and FxCycle Violet Stain (Life Technologies F-10347), respectively, and cells were analyzed on the BD FACSCanto II using FACS Diva software. Viability was assessed by propidium iodide dye exclusion. Trypsinized cells were resuspended in PBS + 1% BSA with 2 µg/mL propidium iodide and analyzed using a BD FACScan.

Senescence-associated β-galactosidase staining and LDH assay for cell death

Cells were plated at a density of 125,000 cells per well of 6-well plates on day 0 with vehicle or 4-OHT treatment. At indicated days following seeding, senescence-associated β-galactosidase activity was detected using previously described methods (Debacq-Chainiaux et al., 2009). LDH was measured using the Roche Cytotoxicity Detection Kit (Roche 11644793001).

Metabolite extraction and analysis

For metabolite analysis using gas chromatography/mass spectrometry, cells were cultured for ~72 h in 6-well plates in glucose- and glutamine-free DMEM (Sigma D5030) containing 10% dialyzed FBS, 1% streptomycin/penicillin, 4 mM glutamine or 25 mM glucose, and the appropriate tracer, [U-$^{13}C_6$]glucose, [U-$^{13}C_5$]glutamine, or [5-^{13}C]glutamine (all from Cambridge Isotopes Laboratories, Inc). After incubation, media was aspirated, and each well was rinsed with 1 ml ice-cold saline. Saline was aspirated, and cells were quenched with 500 µl of -20°C HPLC-grade methanol. 300 µl

of ice-water was added, and cells were scraped with a 1000 µl pipette tip and collected in 1.5 ml Eppendorf tubes. 500 µl of -20°C chloroform was added to each tube and vortexed for 10 min at 4°C. Extracts were centrifuged at 14,000*g* for 5 min at 4°C. The upper aqueous phase was collected in a separate tube evaporated under nitrogen for polar metabolite analysis. The lower layer was collected in a separate tube and evaporated under nitrogen for nonpolar metabolite analysis. Metabolites were derivatized and analyzed using gas chromatography/mass spectrometry as previously described (Fendt et al., 2013; Metallo et al., 2012). The rate of fatty acid synthesis was calculated as previously described (Fendt et al., 2013).

For metabolite analysis using liquid chromatography tandem mass spectrometry (LC-MS/MS), cells were cultured for ~24 h in 10 cm plates. After incubation, media was aspirated, and each plate was rinsed with 10 ml ice-cold saline. Saline was aspirated, and cells were quenched with 2.89 ml of -20°C HPLC-grade methanol. 1.74 ml of ice-water was added, and cells were scraped with a cell lifter and collected in 15 ml conical tubes. 2.89 ml of -20°C chloroform was added to each tube and vortexed for 10 min at 4°C. Extracts were centrifuged at 4,000g for 15 min at 4°C. The upper aqueous phase was collected in a separate tube evaporated under nitrogen for polar metabolite analysis. LC-MS/MS analysis was done using a variation of the method described previously (Munger et al., 2008). A Paradigm MS4 HPLC (Michrom Bioresources, Auburn, CA), and a Synergi Hydro column (4 µm particle size, 80 Å, 150 mm × 2 mm, from Phenomenex) were used for separation of metabolites by polarity. Prior to column separation, samples were loaded onto a trapping column (C18, 4 mm × 2 mm, from Phenomenex) and washed for 30 seconds with HPLC grade water containing 10 mM tributylamine and 15 mM acetic acid for rapid desalting. HPLC separation was coupled with negative-mode electrospray ionization (ESI) to a TSQ Vantage Triple Stage Quadrupole Mass Spectrometer (Thermo Scientific) operating in multiple reaction monitoring (MRM) mode. The LC parameters were as follows: autosampler temperature, 10 ºC; injection volume, 10 µl; column temperature, room temperature; and flow rate, 200 $\mu l \cdot min^{-1}$. The LC solvents were Solvent A: 10 mM tributylamine and 15 mM acetic acid in 97:3 water:methanol (pH 4.95); and Solvent B: methanol. Elution from the column was performed over 50 min with the following gradient: t = 0, 0% B; t = 5, 0% B; t = 10, 20% B; t = 20, 20% B; t = 35, 65% B; t = 38, 95% B; t = 42, 95% B, t = 43, 0% B; t = 50, 0% B. ESI spray voltage was 3,000 V. Nitrogen was used as the sheath gas at 30 psi and as the auxiliary gas at 10 psi, and argon as the collision gas at 1.5 mTorr, with the capillary temperature at 325 ºC. Scan time for each MRM transition was 0.1 s with a scan width of 1 m/z. The LC runs were divided into time segments, with the MRM scans within each time segment containing compounds eluting during that time interval. For compounds eluting near boundaries between time segments, the MRM scan corresponding to the compound was conducted in both time segments. Instrument control, chromatographic control, and data acquisition were performed by the Xcalibar software (Thermo Scientific).

Data analysis was performed using MAVEN (Clasquin et al., 2012; Melamud et al., 2010). Pool sizes were first normalized by total protein of extracted cells. The protein content of extracted cells was determined from the dried protein fraction from each extraction, which was incubated overnight in 2 ml of 0.2 M KOH, and quantified by

Bradford assay. Isotope labeling data was corrected for the natural abundance of different isotopes using IsoCor (Millard et al., 2012).

CO_2 production from glucose

To assay $^{14}CO_2$ production from ^{14}C-labeled glucose, cells were incubated in 5 $\mu Ci \cdot ml^{-1}$ uniformly labeled (American Radiolabeled Chemicals #0122A) glucose for 24 hours. Carbon dioxide was trapped on a tight-fitting piece of Whatman paper that had been saturated with a solution of $Ba(OH)_2$; the resulting reaction between emitted CO_2 and $Ba(OH)_2$ resulted in a barium bicarbonate precipitate that was retained on the paper. The paper overlying each well was counted in 10 ml of scintillation fluid using a Beckman Coulter LS6500 Scintillation Counter. Total $^{14}CO_2$ emission was calculated by subtracting background radioactivity from the radioactivity on the filter paper.

Exogenous PKM1 expression

Standard retroviral infection protocol was used to introduce PKM1 expression constructs or delivery of an empty vector control (pLHCX). Briefly, target cells were incubated in virus-containing media produced from an HEK-293T packaging line for 24 hours. Media was changed and the cells were allowed to recover in standard media for 24 hours before they were incubated with hygromycin (100 µg/mL) for 5 days with daily media changes. During antibiotic selection and proliferation analysis, cells were passaged to a confluence of 750,000 cells per 10 cm plate every 3 days.

Gene expression analysis

Primary MEFs derived from two independent embryos were treated with vehicle or 4-OHT treated as previously described. The growth medium was removed 7 days following vehicle or 4-OHT addition, and cells were lysed on the dish using TRIzol Reagent (Life Technologies); RNA was isolated according to the manufacturer's protocol and RNA pellets were resuspended in DEPC-treated water. Microarray analysis was performed by the MIT BioMicro Center. Briefly, RNA quantity and quality were determined using an Agilent 2100 BioAnalyzer prior to sample preparation and hybridization to an Affymetrix GeneChip Mouse Gene 1.0 ST array. The intensity (.CEL) files were RMA normalized using Affymetrix Expression Console. Unsupervised hierarchical clustering was performed with Cluster 3.0. Genes were filtered based on standard deviation. Genes and arrays were centered at the mean prior to clustering genes and arrays using complete linkage methods and the correlation (uncentered) similarity metric. Probe identifiers were converted to gene names using DAVID (Huang et al., 2008, 2009). Clustering results were visualized with JavaTreeView. Figures were converted to a full-spectrum color scale using Matlab. Fold change analysis was conducted using Significance Analysis of Microarrays tool (Tusher et al., 2001) featured in the MuliExperiment Viewer within the TM4 Microarray Software Suite (Saeed et al., 2003). Microarray data are available on Gene Expression Omnibus (GEO), accession number GSE60499.

Retroviral Infection

A standard retroviral infection protocol was used to introduce expression constructs for PKM1 or an empty vector control (pLHCX). Briefly, HEK-293T cells were incubated for

36 hours in media containing 3 μg of the EcoPak packaging DNA and 3 μg of the vector of interest. Target cells were then incubated in the virus-containing media for 24 hours. Media was changed and the cells were allowed to recover in standard media for 24 hours before they were incubated with hygromycin (100 μg/mL) for 5 days with daily media changes. During antibiotic selection and proliferation analysis, cells were passaged to a confluence of 750,000 cells per 10 cm plate every 3 days.

RNA

RNA was isolated from *PKM2*$^{fl/fl}$ and *PKM2*$^{\Delta/\Delta}$ MEFs derived from *PKM2*$^{fl/fl}$ *Cre-ER* embryos 7 days following vehicle or 4-OHT addition using the Qiagen RNeasy Mini Kit (Qiagen 74104). Quantitative RT-PCR was performed using the QuantiTect SYBR Green RT-PCR kit (Qiagen 204243). Primer sequences for RT-PCR were the following:

Actin-F: CATCATGCGTCTGGACCTG
Actin-R: CTCACGTTCAGCTGTGGTCA

CAD-F: CGTGGAGACCATTGAACTGA
CAD-R: GCCTGAGCCTGTTCAAGAGA

CPT1-F: TCAAGAATGGCATCATCACTG
CPT1-R: GGAGGGGTCCACTTTGGTAT

H6PD-F: GCAGGTGTCCTTGTCCACAT
H6PD-R: ACGCCCGATTCTTAAACACA

HMCN1-F: TGTGAATGAAGATGCTGGTGA
HMCN1-R: TTCCACTGGCTCAAGAGTGA

IFI44-F: AACATGGCATTCTGCATTTG
IFI44-R: AATGCCTCCAGCTTGGACTT

IFIT1-F: ATGGGAGAGAATGCTGATGG
IFIT1-R: GAGATTCTCACTTCCAAATCAGG

PPAT-F: GAAGACCAAATGGTTTATACAGTAAGG
PPAT-R: CAGGCGTAGCAGACTCTGGA
TKT-F: TCACAGGGATTGAAGACAAGG
TKT-R: GGCCAGGATCTTCTTTTTGC.

Statistical analyses

Data are presented as means ± standard error of the mean (SEM). All *P* values were obtained using an unpaired two-tailed *t*-test, and statistical significance was determined at a value of 0.05.

13C-Metabolic flux analysis model included as Excel file.

Intracellular fluxes where modeled with the MatLab based software Metran (Antoniewicz et al., 2007; Young et al., 2008).

The flux model contains the following assumptions:

- Fluxes were modeled based on intracellular labeling of lactate, alanine, citrate, a-ketoglutarate, fumarate, malate, aspartate, glutamate, glutamine
- The system is in steady state. Unpublished data confirm that there is no significant difference in the labeling of polar metabolites after 24h or 72h
- All CO2 in the system is unlabeled
- Fumarate and succinate have no orientation, because they are symmetrical
- Any metabolite that is modeled in two different compartments is in equilibrium
- Entry of unlabeled pyruvate and AcCoA precursors is possible. Which is possible due to fatty acid oxidation or entry of amino acids from the media
- Flux to fatty acids is not constrained
- 3PG to serine flux was estimated with a specific serine/glycine flux model
- Biomass fluxes were based on Metallo et al 2009. The biomass fluxes were scaled for the total protein content of PKM1 and PKM2 cells and the measured growth rates
- Flux magnitude to NTPs was based on Metallo et al 2009 and scaled by EdU incooperation into DNA
- Pentose phosphate pathway flux was modeled as lower bound based on the flux to NTPs
- Glutamine to glutamate flux was calculated based on dynamic labeling data (Yuan et al., 2008).

Specific assumptions for serine/glycine model:

- Fluxes were modeled based on serine and glycine labeling
- Metran does not allow constraining net fluxes, therefore a forward flux for serine/glycine entry into the cell was modeled, while the reverse flux was modeled as serine/glycine sink. The difference of the forward and revers flux is the net flux, which was measured as serine/glycine uptake rate.

References

Antoniewicz, M.R., Kelleher, J.K., and Stephanopoulos, G. (2007). Elementary metabolite units (EMU): a novel framework for modeling isotopic distributions. Metabolic engineering *9*, 68-86.

Clasquin, M.F., Melamud, E., and Rabinowitz, J.D. (2012). LC-MS Data Processing with MAVEN: A Metabolomic Analysis and Visualization Engine. In Current Protocols in Bioinformatics (John Wiley & Sons, Inc.).

Debacq-Chainiaux, F., Erusalimsky, J.D., Campisi, J., and Toussaint, O. (2009). Protocols to detect senescence-associated beta-galactosidase (SA-[beta]gal) activity, a biomarker of senescent cells in culture and in vivo. Nat. Protocols *4*, 1798-1806.

Fendt, S.-M., Bell, E.L., Keibler, M.A., Olenchock, B.A., Mayers, J.R., Wasylenko, T.M., Vokes, N.I., Guarente, L., Heiden, M.G.V., and Stephanopoulos, G. (2013). Reductive glutamine metabolism is a function of the α-ketoglutarate to citrate ratio in cells. Nat Commun *4*.

Huang, D.W., Sherman, B.T., and Lempicki, R.A. (2008). Systematic and integrative analysis of large gene lists using DAVID bioinformatics resources. Nat. Protocols *4*, 44-57.

Huang, D.W., Sherman, B.T., and Lempicki, R.A. (2009). Bioinformatics enrichment tools: paths toward the comprehensive functional analysis of large gene lists. Nucleic Acids Research *37*, 1-13.

Melamud, E., Vastag, L., and Rabinowitz, J.D. (2010). Metabolomic Analysis and Visualization Engine for LC−MS Data. Analytical Chemistry *82*, 9818-9826.

Metallo, C.M., Gameiro, P.A., Bell, E.L., Mattaini, K.R., Yang, J., Hiller, K., Jewell, C.M., Johnson, Z.R., Irvine, D.J., Guarente, L.*, et al.* (2012). Reductive glutamine metabolism by IDH1 mediates lipogenesis under hypoxia. Nature *481*, 380-384.

Millard, P., Letisse, F., Sokol, S., and Portais, J.-C. (2012). IsoCor: correcting MS data in isotope labeling experiments. Bioinformatics *28*, 1294-1296.

Munger, J., Bennett, B.D., Parikh, A., Feng, X.J., McArdle, J., Rabitz, H.A., Shenk, T., and Rabinowitz, J.D. (2008). Systems-level metabolic flux profiling identifies fatty acid synthesis as a target for antiviral therapy. Nat Biotechnol *26*, 1179-1186.

Rando, T.A., and Blau, H.M. (1994). Primary mouse myoblast purification, characterization, and transplantation for cell-mediated gene therapy. The Journal of Cell Biology *125*, 1275-1287.

Saeed, A., Sharov, V., White, J., Li, J., Liang, W., Bhagabati, N., Braisted, J., Klapa, M., Currier, T., and Thiagarajan, M. (2003). TM4: a free, open-source system for microarray data management and analysis. Biotechniques *34*, 374.

Springer, M.L., Rando, T.A., and Blau, H.M. (2001). Gene Delivery to Muscle. In Current Protocols in Human Genetics (John Wiley & Sons, Inc.).

Tusher, V.G., Tibshirani, R., and Chu, G. (2001). Significance analysis of microarrays applied to the ionizing radiation response. Proceedings of the National Academy of Sciences *98*, 5116-5121.

Young, J.D., Walther, J.L., Antoniewicz, M.R., Yoo, H., and Stephanopoulos, G. (2008). An elementary metabolite unit (EMU) based method of isotopically nonstationary flux analysis. Biotechnol Bioeng *99*, 686-699.

Yuan, J., Bennett, B.D., and Rabinowitz, J.D. (2008). Kinetic flux profiling for quantitation of cellular metabolic fluxes. Nat Protoc *3*, 1328-1340.